DSMC Dusty Flow Simulation for Non-stop Mars Sample Return Mission

T. Ozawa, T. Suzuki, H. Takayanagi, and K. Fujita

*Aerospace Research and Development Directorate
Japan Aerospace Exploration Agency,
Chofu, Tokyo 182-8522 JAPAN

Abstract. At Japan Aerospace Exploration Agency, a non-stop Mars sample return project has been planned. In the project, sampling of Martian dust particles is planned between 35 and 45 km, and the impact of Martian dust particles on a shock structure and aerodynamics for a spacecraft must be clarified. In this work, a mechanism for hypersonic dusty flow simulations in DSMC has been developed, and hypersonic dusty flows were simulated for clear weather and dust storm conditions using two dust-surface interaction models at the descent altitude. It was found that although the impact of dust particles on the shock structure and drag is negligible, the total heat flux is increased with the consideration of dust particles.

Keywords: Mars, Dust, Heat Transfer, Martian Atmosphere, DSMC, MASC

INTRODUCTION

In May 2003, the Institute of Space and Astronautical Science (ISAS) of Japan launched the Hayabusa spacecraft [1] toward Asteroid 1998SF36 Itokawa, and it succeeded in coming back to the earth in June 2010. To continue the success of Japanese aerospace exploration and science technology, the Mars Exploration with Lander-Orbiter Synergy (MELOS) mission has come under review in Japan Aerospace Exploration Agency (JAXA) together with a lot of planetary scientific groups all over Japan. As one of the MELOS projects, a non-stop Mars sample return project, named Mars Aero-flyby Sample Collection (MASC) [2], has been planned in our group. In this project, a sphere-cone shape spacecraft [3] enters the Martian atmosphere and the descent altitude for the Martian dust sampling is considered to be between 35 and 45 km altitudes. In Ref. [4], the dust particle size distributions between 35 and 45 km altitudes for the average and storm weather cases were investigated, and it was found that the Martian dust concentration is sensitive to the weather condition, and the number density for the storm condition is increased by approximately two orders of magnitude compared to the average condition. For the success of the project, the accurate estimation of the Martian dust influences on the spacecraft aerodynamics and heat shield during the Martian atmosphere entry is crucial, especially when we utilize the aero-capture technologies [2].

Previously, several groups have studied the effect of dust particles on heat shield of Mars entry vehicles. Papadopoulos *et al.* [5] predicted a significant surface erosion at 40 km altitude for a 70 degree half-angle, 26m-diameter blunt cone with a 8.6 km/s speed. On the other hand, Palmer *et al.* [6] concluded that the dust effect is negligible on the Mars 2001 Lander vehicle. Migita *et al.* [7] demonstrated the Eulerian and Lagrangian hybrid approach to simulate supersonic dusty flows over a 1-m sphere. Using an unrealistic dust mass loading ratio of 0.5 in the Martian atmosphere, they presented the effect of dust particles on the shock-layer thickness, drag and heat transfer rate. Because the effect of dust particles on aerodynamics of a Mars entry vehicle depends on the shape and the size of the vehicle as well as the trajectory of the mission, it is not well-known whether the presence of dust particles can cause the change of the shock structure and aerodynamics for the MASC vehicle. Therefore, in this work the effect of micron-size dust particles on the MASC spacecraft aerodynamics has been investigated for Martian atmosphere entry at 45 km, which is a planned descent altitude in the project. At this altitude, the continuum assumption may not be applicable for the hypersonic bow-shock flows due to the breakdown effect, and thus, the direct simulation Monte Carlo (DSMC) method is employed. In our earlier work [4], the drag and heat transfer on a micron-size dust particle between 1 μm and 10 μm has been investigated macroscopically and microscopically during traveling through a hot-temperature shock between 35 and 45 km. It was found that the microscopic DSMC heat transfer results agree better with the Koshmarov and Svirshevskii (K-S) [8] and free-molecule (F-M) [9] models than the modified Kavanau model [10]. Utilizing the information of the particle drag and heating, a mechanism in DSMC computations for hypersonic dusty flows has been developed, and the impact of dust particles on the shock structure and aerodynamics for the MASC vehicle has been assessed.

MODELING OF MARTIAN DUSTY FLOWS IN DSMC

At JAXA, a new DSMC code, named modeling of transitional-ionized flows (MOTIF), has been developed to simulate rarefied nozzle flows or planetary atmospheric flows. The new code follows the fundamentals of the rarefied reacting atmosphere code (RARAC), and the details of the code can be found in Ref. [11]. In the code, both neutral and charged species can be simulated, and for charged species, a single-time step ion-averaged velocity (IAV) model [12] is utilized. The no time counter (NTC) scheme [13] is employed for modeling the molecular collision frequency, and the variable hard sphere (VHS) [13] model is used for modeling the collision cross section between particles. The Borgnakke-Larsen (BL) model with temperature-dependent rotational and vibrational relaxation numbers is used for modeling rotation-translation (R-T) and vibration-translation (V-T) energy transfers between neutral species. The Millikan and White (MW) form of the relaxation time are used for V-T rates, and Parker's rates for the R-T rates. For modeling chemical reactions the total collision energy (TCE) [13] model is used. For the gas-surface interaction modeling, both the Maxwell reflection model and Cercignani-Lampis-Lord (CLL) reflection model are employed.

In this work, the code has been modified to simulate Martian gas-dust two-phase flows. First of all, the scale and the number density of atmospheric gas and dust particles are so different that two different F_{num} for gas and dust are employed in our code. F_{num} is a number of real molecules represented by a DSMC particle, and in a two dimensional axisymmetric (2D-AX) code this depends on the radial coordinate, r. Secondly, gas-dust collisions are modeled so that the effect of dust particles on gas shock structure and drag and heat transfer for the capsule has been investigated. Note that although the gas-dust interaction is considered, the collisions between dust particles are not modeled because the impact of the dust-dust collisions is not important due to the low number density for the MASC project condition. The number of collisions $N_{col(p-d)}$ between a dust particle and gas particles are calculated as follows.

$$N_{col(p-d)} = n_p \overline{\sigma v_r} \Delta t_d F_{num,d}(r) \tag{1}$$

where subscripts p and d denote a DSMC gas particle and dust particle, respectively. In the dusty flow simulations, two time steps for the movement of gas and dust particles are introduced, which are based on the collision frequency between gas particles and that between dust and gas particles, respectively. Because the ratio of number of collisions between gas and a dust particle to the number of DSMC gas particles inside a cell is so high that a weighting collisional factor W_c is introduced as follows.

$$\Delta q = \sum_{i}^{N_{col}} (E_{col,i}^{post} - E_{col,i}^{pre}) = \sum_{i}^{N_{col}/W_c} W_c (E_{col,i}^{post} - E_{col,i}^{pre}). \tag{2}$$

W_c is employed when the ratio is so high and is determined so as to maintain the statistical number of sampling for drag and heat transfer between a dust particle and gas during a time step. The selection of a colliding gas particle is the same way as the general DSMC collision mechanism in the MOTIF code. After a collision pair is selected, the energy and momentum of a dust particle are always updated whereas the properties of a gas particle are updated only if the probability of the acceptance for the change of gas particle properties per each collision is greater than a random number. The probability is calculated as $P_r = \frac{W_c}{F_{num,p}(r)}$. The pre- and post- collisional energies are calculated as

$$\begin{aligned} E_{col,p}^{pre} &= \frac{1}{2} m_r v_r^2 + E_{rot,p} + E_{vib,p}, \quad E_{col,p}^{post} = \frac{1}{2} m_r (v_r^{post})^2 + E_{rot,p}(T_d) + E_{vib,p}(T_d), \\ v_r^{post} &= \sqrt{\frac{2k_B T_d}{m_p} [-\ln(Rn_1 Rn_2)]}. \end{aligned} \tag{3}$$

The gas-dust surface interaction was modeled using the Maxwell model, and a diffuse condition with total energy and momentum accommodation with the dust surface temperature was assumed. Using the VHS model and the conservation of momentum, the post-collisional velocities are

$$\mathbf{v}_d = \mathbf{v}_{CM} - \frac{m_p}{m_p + m_d} \mathbf{v}_r^{post}, \quad \mathbf{v}_p = \mathbf{v}_{CM} + \frac{m_d}{m_p + m_d} \mathbf{v}_r^{post}. \tag{4}$$

The change of momentum of a dust particle depends on the W_c, and the post-collisional velocity of a gas particle is accepted if $Rn < P_r$. The change of temperature of the dust particle, ΔT_d is also calculated as

$$\Delta T_d = \Delta q / (m_d c_d) \times f_{Tad}, \tag{5}$$

where $f_{Tad} = T_{ad}/T_g$. The adiabatic temperature T_{ad} (or recovery temperature) is calculated as $T_{ad} = \left(\frac{\gamma-1}{\gamma}M^2 f_r + 1\right)T_g$, where f_r is the recovery factor. In Ref. [14], the recovery factor was assumed as $f_r = \sqrt{Pr}$. The details of dust particle heating traveling through a shock have been examined in Ref. [4], and it was found that f_{Tad} is approximately 1.7 inside the shock.

In this work, 8 species (N, O, C, N_2, O_2, NO, CO, CO_2) were considered in the Martian gas flow. Totally, 54 chemical reactions including 40 dissociation reactions were considered in the calculation [15]. The gas-surface interaction was modeled using the Maxwell model with total energy and momentum accommodation with a surface temperature of 500 K. The time step, cell size, computational domain, and total number of simulated molecules were investigated to obtain results that are independent of these DSMC numerical parameters.

RESULTS AND DISCUSSION

Dust Heating in DSMC

In DSMC, a dust particle was inserted near the stagnation line, and the drag force and energy transfer was calculated being based on the gas-dust particle interaction. Three cases are compared in this work, and each condition is listed in Table 2. The viscosity index of a dust, ω_d, was assumed to be 0.5 (hard sphere model), and different ω for a gas-dust pair and f_{Tad} were tested. The radius of a dust particle r_d is set to 1 μm in Fig. 1. For case (a), the hard sphere model was employed and the DSMC results was found to overestimate the dust heating compared to the results obtained by the macroscopic models. For case (b), the VHS model with $\omega = (\omega_g + \omega_d)/2$ was used, and without considering f_{Tad}, the dust heating was found to be underpredicted. For case (c), the same ω as case (b) and $f_{Tad} = 1.7$ were used, and good agreement with the K-S and F-M models can be seen in the figure. Note that the modified Kavanau, which is the simplest macroscopic model, estimates lower dust heating than the other models. Thus, for the gas-dust collision model, the parameters used for case (c) are to be employed in the following results. In Fig. 2, the heating of a 1 μm dust particle off the stagnation line is presented. It can be seen that the DSMC results agree well with the K-S and F-M models for both trajectories of $r = 10$ and 20 cm. The dust size dependence was also investigated, and in Fig. 3 a comparison of a dust particle heating along the stagnation trajectory between the macroscopic 3 models and DSMC calculations for r_d =2 and 10 μm is shown. A 2-μm particle can be heated up to approximately 380 K, and good agreement is obtained among DSMC, K-S and F-M models. For a 10-μm particle, the maximum temperature is only 210 K, and three results agree well whereas the Kavanau model predicts slightly lower temperature.

Dusty Flows in DSMC

In the previous subsection, the gas-dust collision model for the Mars entry at 45 km was investigated, and in this subsection, using the recommended collision model, Martian dusty flows were simulated so as to evaluate the effect of micron size dust particles on the shock structure and aerodynamics on the spacecraft. In our code, since one size dust particle can be considered, the radius of dust particles is specified to be 1 μm based on the dust particle size distribution (see Ref. [4]). Also, from the distribution, the dust mass loading ratio, η, for a clear weather condition and a dust storm condition was estimated, and in this work, η_{cl} and η_{st} were set to 10^{-4} and 10^{-2}, respectively. Subscripts *cl* and *st* represents a clear weather and a dust storm, respectively. The corresponding 1 μm dust number density, n_d, was approximately computed, and $n_{d,cl} = 1 \times 10^6$ and $n_{d,st} = 1 \times 10^8$ m^{-3} were utilized on the assumption of a clear weather and a dust storm condition. Furthermore, two dust reflection models were employed for the reflection on the capsule. One is a 100% sticking condition, and another is a 100 % specular reflection condition.

In Fig. 4, comparisons of v_x contours between the cases with and without Martian dusts at 45 km are shown. The top figure is the case for $n_d = 1 \times 10^6$ m^{-3}, and the bottom is the case for 1×10^8 m^{-3}. The effect of micron dust particles on the shock structure can hardly be seen for both cases. The similar feature on the temperature distributions is presented in Fig. 5. In Figs. 6 and 7, distributions of drag and heat transfer coefficients between the Martian dust and total (gas and dust) along the spherecone body at 45 km with $n_d = 1 \times 10^6$ and 1×10^8 m^{-3} are compared. For the 100 % sticking case. because the dust particles are rarely decelerated by the shock, the C_D (dust) is approximately uniform along the surface. The drag ratio of dust particles to the total is approximately the same as the dust mass loading ratio. On the other hand, the heat transfer ratio is higher than the dust mass loading ratio, and it is approximately 0.001 and 0.12 for $n_d = 1 \times 10^6$ and 1×10^8 m^{-3} cases, respectively. Thus, for the dust storm condition, the total heat flux is increased by 12 % with the consideration of dust particles.

For the 100 % specular wall case, C_D (dust) is approximately doubled at the stagnation point, and the increase rate of the dust drag contribution is smoothly decreased as the reflection angle decreases in the downstream. Although the contribution of the dust drag is increased, the change in the total drag is less than a few percent even for the dust storm condition. Note that the dust heat transfer coefficient is zero for the specular condition. Namely, the effect of micron-size dust particles for both clear weather and dust storm cases was found to be negligibly small using the specular wall condition.

CONCLUSIONS

A scheme for hypersonic dusty flow simulations in DSMC has been developed, and the impact of dust particles on the shock structure and aerodynamics for the MASC vehicle has been investigated at the descent altitude, 45 km. The gas-dust collision model was analyzed, first, by comparing with the K-S and F-M models, and it was found that the VHS model using the adiabatic temperature ratio of 1.7 is efficient and provides good agreement with the macroscopic models. Hypersonic dusty flows were simulated for clear weather and dust storm conditions using two dust-surface interaction models. In the course of my argument, it should have become clear that the impact of dust particles on the shock structure cannot be observed at 45 km. It was also found that the impact on the drag is negligibly small. Meanwhile, the total heat flux can be increased by 12 % with the consideration of dust particles for the dust storm condition. For our future work, the improvement of the investigation will be carried out. DSMC dust particles will be generated according to the dust size distribution function, and the effect of variance in the particle size will be examined. Moreover, the modeling of the dust-surface interaction will be improved. Finally, hypersonic dusty flow simulations will be extended to 35 km, which is the lowest target altitude in the MASC project.

REFERENCES

1. Kawaguchi, J., Uesugi, T., Fujiwara, A., and Matsuo, H., "The MUSES-C, World's First Sample and Return Mission from near Earth Asteroid:NEREUS," *Acta Astronautica*, Vol. 39, No. 1-4, 1996, pp. 15–23.
2. Fujita, K., Tachibana, S., Sugita, S., Miyamoto, H., Mikouchi, T., Suzuki, T., Takayanagi, H., Ozawa, T., Kawaguchi, J., and Woo, H., "Preliminary Study of Nonstop Mars Sample Return System Using Aerocapture Technologies," AIAA paper 2009-5614, AIAA Atmospheric Flight Mechanics Conference, Chicago, Illinois, August 10 - 13, Aug. 2009.
3. Takayanagi, H., Suzuki, T., and Fujita, K., "Feasibility Assessment of Nonstop Mars Sample Return System," AIAA paper 2010-0627, 48th AIAA Aerospace Sciences Meeting and Exhibit, Orlando, FL, Jan 4-7, Jan. 2010.
4. Ozawa, T., Suzuki, T., Takayanagi, H., and Fujita, K., "Modeling of Martian Dust Collection for Non-stop Mars Sample Return Mission," AIAA paper 2010-0886, 48th AIAA Aerospace Sciences Meeting Including the New Horizons Forum and Aerospace Exposition, Orlando, Florida, Jan. 4-7, 2010, Jan. 2010.
5. Papadopoulos, P., Tauber, M. E., and Chang, I.-D., "Heatshield Erosion in a Dusty Martian Atmosphere," *Journal of Spacecraft and Rockets*, Vol. 30, No. 2, 1993, pp. 140–151.
6. Palmer, G., Chen, Y. K., Papadopoulos, P., and Tauber, M., "Reassessment of Effect of Dust Erosion on Heatshield of Mars Entry Vehicle," *Journal of Spacecraft and Rockets*, Vol. 37, No. 6, 2000, pp. 747–752.
7. Migita, S. and Suzuki, K., "Numerical Analysis on Dusty Supersonic Shock Layer Flow over a Blunt Body," *Journal of the Japan Society for Aeronautical and Space Sciences*, Vol. 49, No. 566, March 2001, pp. 63–69, in Japanese.
8. Koshmarov, Y. A. and Svirshevskii, S. B., "Heat Transfer from a Sphere in the Intermediate Dynamics Region of a Rarefied Gas," *Fluid Dynamics*, Vol. 7, No. 2, 1972, pp. 343–346.
9. Sauer, F. M., "Convective Heat Transfer from Spheres in a Free-Molecule Flow," *Journal of the Aeronautical Sciences*, Vol. 18, No. 5, 1951, pp. 353–354.
10. Kavanau, L. L., "Heat Transfer from Spheres to a Rarefied Gas in Subsonic Flow," *ASME Trans.*, Vol. 77, No. 5, 1955, pp. 617–623.
11. Ozawa, T., Suzuki, T., and Fujita, K., "Experimental and Numerical Studies of Hypersonic Flows in the Rarefied Wind Tunnel," AIAA paper 2010-4513, 10th AIAA/ASME Joint Thermophysics and Heat Transfer, Chicago, Illinois, June 28-July 1, 2010, June 2010.
12. Ozawa, T., Zhong, J., and Levin, D. A., "Development of Kinetic-based Energy Exchange Models For Non-Continuum, Ionized Hypersonic Flows," *Physics of Fluids*, Vol. 20, No. 4, 2008, 046102.
13. Bird, G. A., *Molecular Gas Dynamics and the Direct Simulation of Gas Flows*, Clarendon, Oxford, England, U.K., 1994.
14. Nelson, H. F. and Fields, J. C., "Heat Transfer in Two Phase Solid Rocket Plumes," AIAA paper 1995-2131, 30th AIAA Thermophysics Conference, San Diego, CA, June 19-22, June 1995.
15. Hash, D. B. and Hassan, H. A., "Monte Carlo Simulation of Entry in the Martian Atmosphere," *Journal of Thermophysics and Heat Transfer*, Vol. 7, No. 2, 1993, pp. 228–232.

TABLE 1. Mars entry conditions

Altitude	45 km
n_∞, m^{-3}	1.6×10^{21}
T_∞, K	152.67
v_∞, km/s	5.0
CO_2	0.971
N_2	0.027
Ar	0.0
O_2	0.0017
CO	0.0007

TABLE 2. Gas-Dust particle interaction parameters

Case	ω	f_{Tad}
(a)	0.5	1.0
(b)	$(\omega_g + \omega_d)/2$	1.0
(c)	$(\omega_g + \omega_d)/2$	1.7

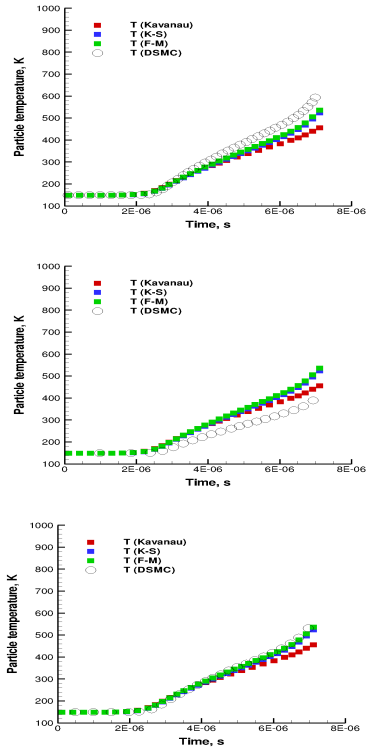

FIGURE 1. Comparisons of a dust particle ($r_d = 1\ \mu$m) temperature change at 45 km between the 3 macroscopic models and DSMC; case a (top), case b (middle) and case c (bottom).

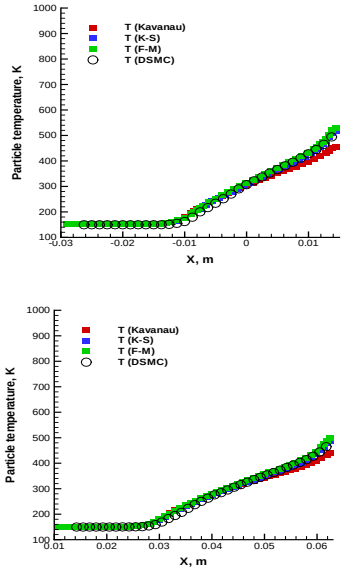

FIGURE 2. Comparisons of a dust particle ($r_d = 1\ \mu$m) heating along the trajectory at $r = 10$ (top) and 20 (bottom) cm between the macroscopic 3 models and DSMC.

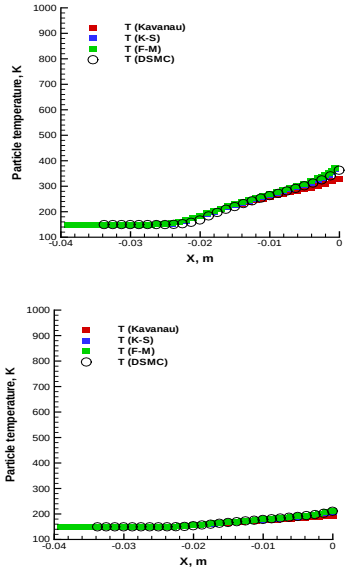

FIGURE 3. Comparisons of a dust particle heating along the trajectory at $r = 0$ cm between the macroscopic 3 models and DSMC for r_d =2 (top) and 10 (bottom) μm, respectively.

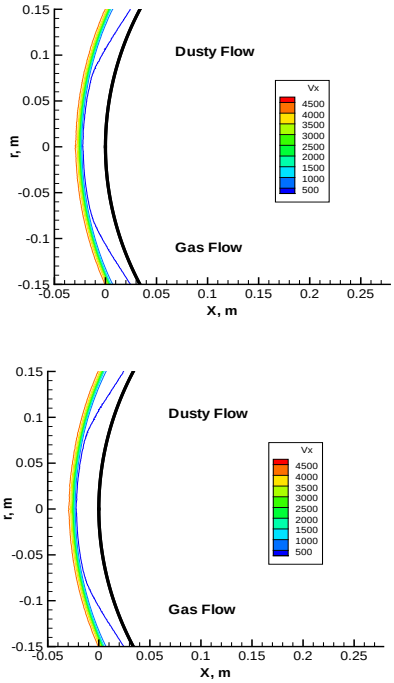

FIGURE 4. Comparisons of v_x contours between the cases with and without Martian dust at 45 km altitude for $n_d = 1 \times 10^6$ (top) and 1×10^8 (bottom) m^{-3}, respectively.

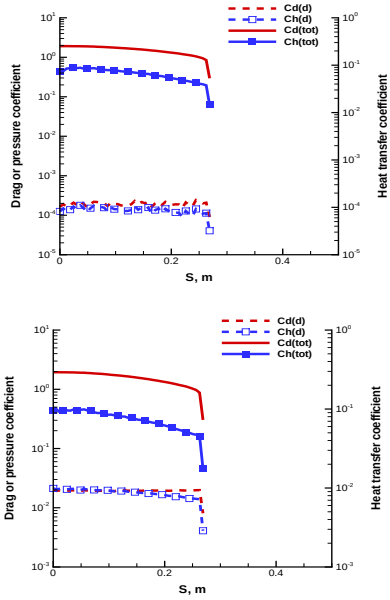

FIGURE 6. Distributions of drag and heat transfer coefficients of the Martian dust and total (gas and dust) along the spherecone body at 45 km with $n_d = 1 \times 10^6$ (top) and 1×10^8 (bottom) m^{-3} (with the sticking condition).

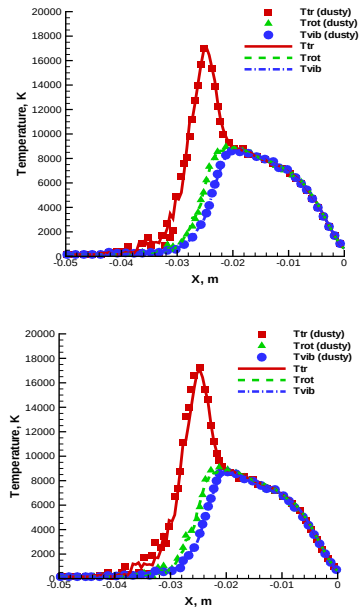

FIGURE 5. Comparisons of distributions of translational, rotational and vibrational temperatures along the stagnation line at 45 km between cases of gas flow only (lines) and dusty flow (symbols) with $n_d = 1 \times 10^6$ (top) and 1×10^8 (bottom) m^{-3}.

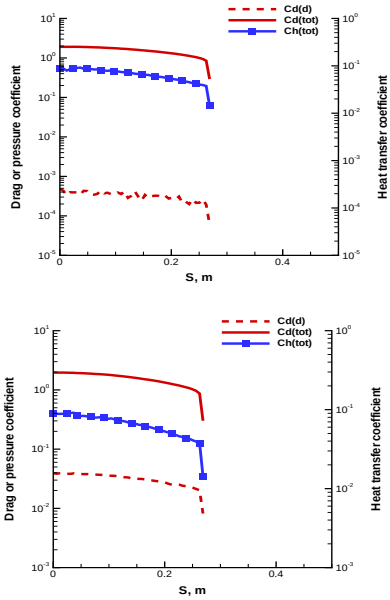

FIGURE 7. Distributions of drag and heat transfer coefficients of the Martian dust and total (gas and dust) along the spherecone body at 45 km with $n_d = 1 \times 10^6$ (top) and 1×10^8 (bottom) m^{-3} (with the specular reflection).